Supporting Information

Elastic *a*-Silicon Nanoparticles Backboned-Graphene Hybrid as a Self-Compacting Anode for High Rate Lithium-Ion Batteries

Minseong Ko, Sujong Chae, Sookyung Jeong, Pilgun Oh, and Jaephil Cho*

School of Energy and Chemical Engineering, Ulsan National Institute of Science and Technology (UNIST), Ulsan 689-798, South Korea

***Address correspondence to**

jpcho@unist.ac.kr

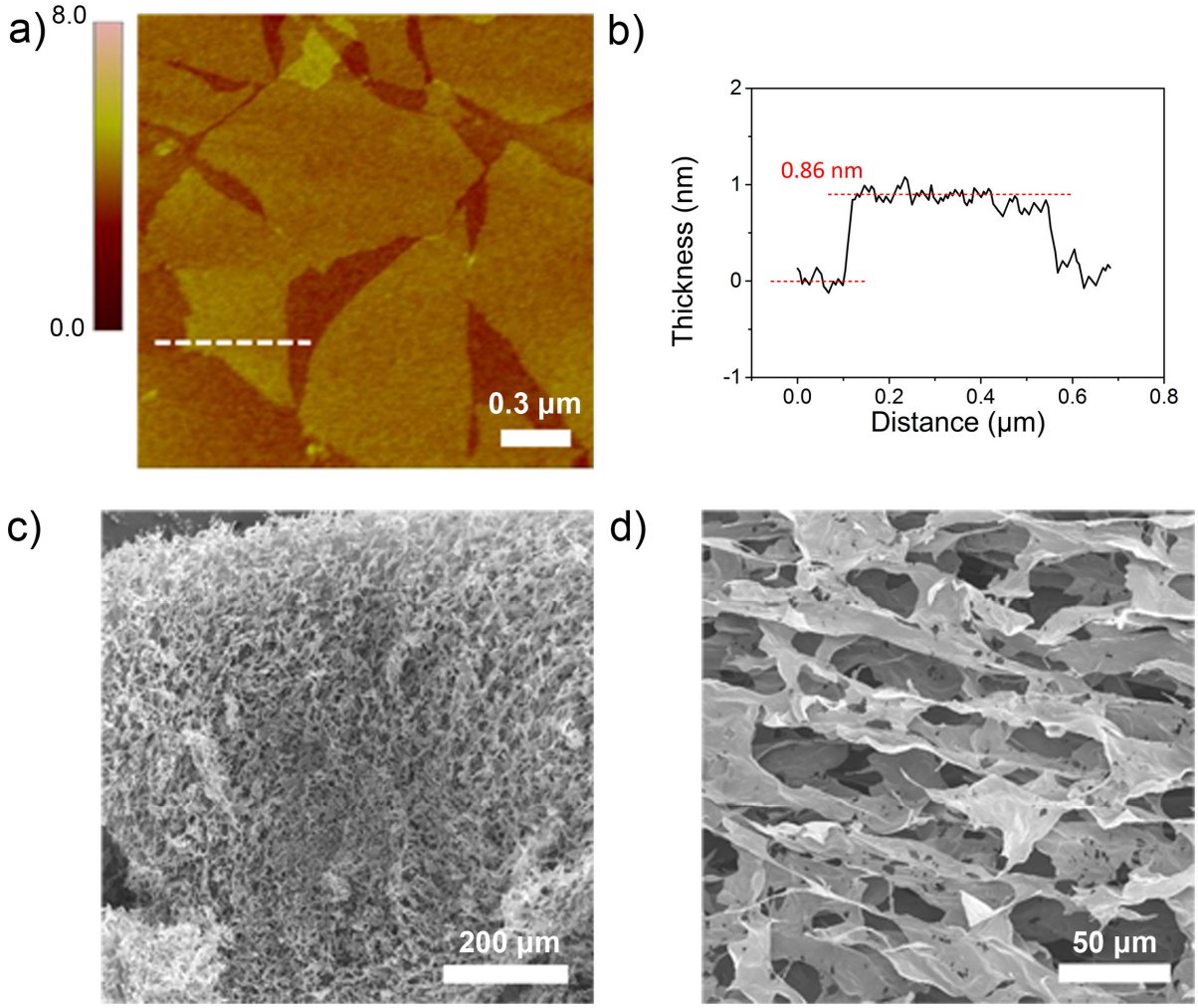

Figure S1. The morphology of as-prepared graphene oxide (GO) and reduced graphene oxide (rGO). a) A tapping mode AFM image of GO sheets, b) the height profile of the AFM image, and c) SEM images of 3D porous rGO with low and d) high magnification *via* freeze-drying[1] followed by thermal reduction process at 1000 °C for 1 hour under a hydrogen atmosphere. This SEM image shows formation of loosely interconnected graphene sheets with large number of macropores.

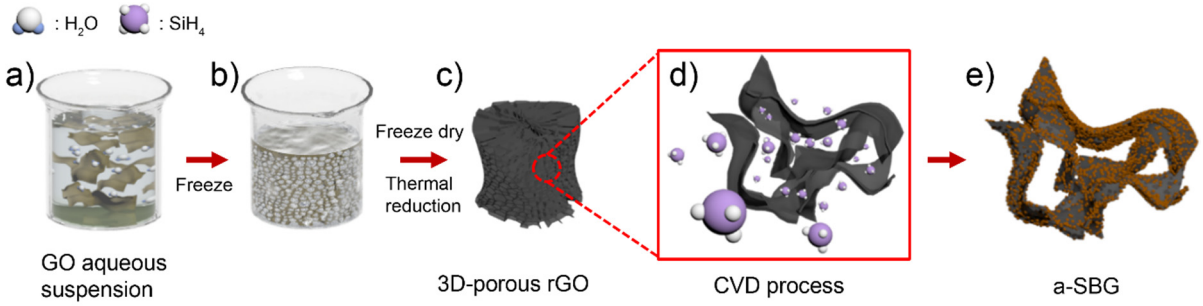

Figure S2. Schematic of fabrication process (a-e) for *a*-SBG nanocomposites. a) GO aqueous suspension prepared by modified hummer's method. b) GO aqueous suspension is then frozen, c) freeze-dried and thermally reduced at 1000 °C, consequently forming 3D porous rGO. d) By facile penetration and decomposition of silane (SiH_4) gas into individual rGO surface at 550 °C during 30min, e) amorphous Si nanoparticles backboned-graphene nanocomposites (*a*-SBG) are eventually synthesized.

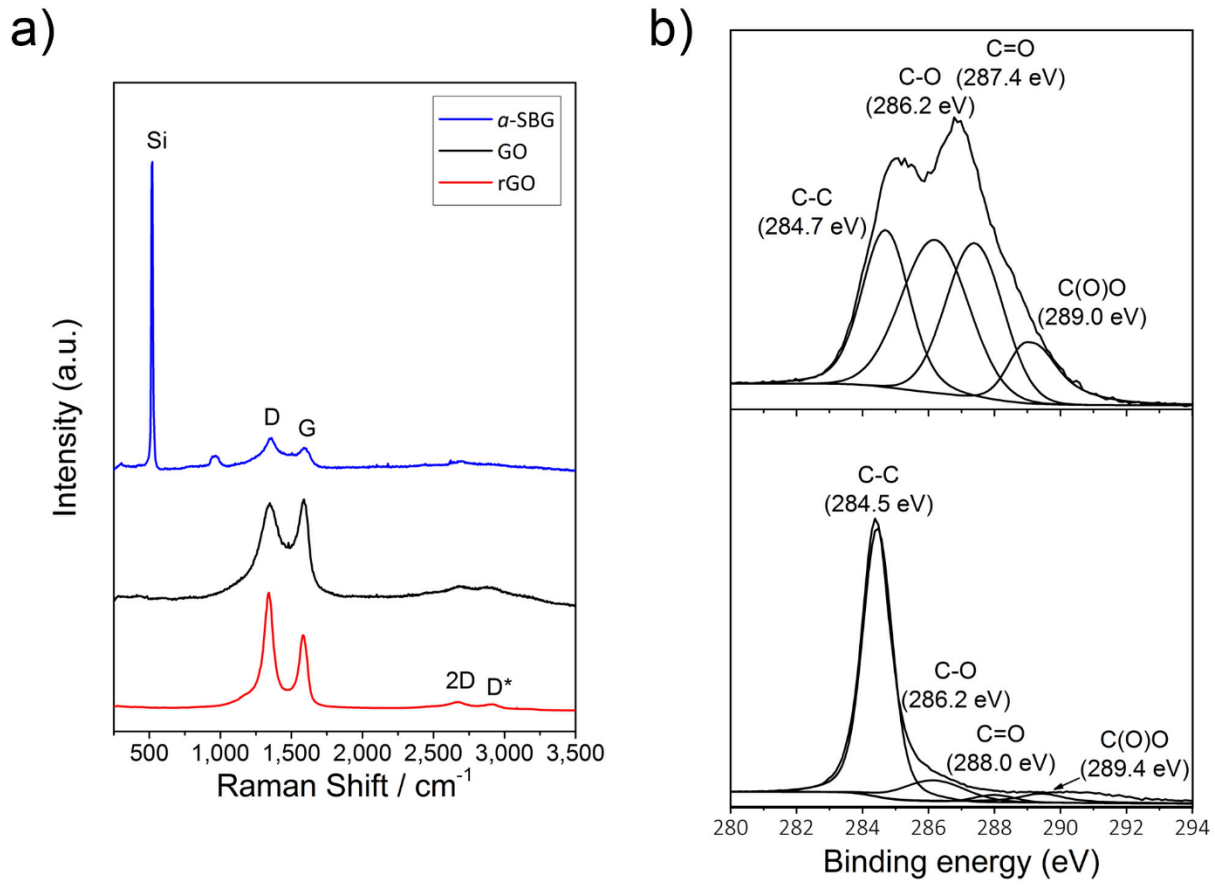

Figure S3. a) Raman spectra analysis of GO, rGO and *a*-SBG. b) XPS C 1s spectra of GO and rGO, respectively.

Raman spectroscopy was conducted for characterizing the graphitic materials. All the samples exhibited different intensity and wavenumbers with three main peaks indicating G and D peak, and the second order of 2D peak. The graphene oxide synthesized by modified Hummers method clearly revealed the disorder-induced D peak with prominent intensity at ~1350 cm^{-1} comparable with broaden graphitic G peak at ~1598 cm^{-1}, with relatively small intensity of the 2D peak at ~2700 cm^{-1}, which indicates significant structural disorder by heavy oxidization. The thermally reduced GO (rGO) spectrum presents a little shift back of G peak with respect to that of GO. It reflects the recovery of hexagonal carbon network with the mitigation of

oxygen-defects. The silicon deposited graphene appears the high intensity of silicon peak at ~521 cm^{-1} with decline of carbon peaks, which result well verified the silicon deposition on rGO sample. X-ray photoelectron spectroscopy (XPS) surveys confirmed the successful reduction of GO to rGO with severe decrease of oxygen functionalities. The high-resolution C1s spectrum exhibited the well-defined double peak formations, which means extreme oxidized GO. However, after thermal reduction the C1s spectrum presents a transformation from a double peak to a single sharp peak by shifting the maximum peak back to ~284.5eV, indicating the progressive restoration of sp2 bonding in reduced graphene oxide results in achieving the electrical conductivity from insulated GO.[2, 3]

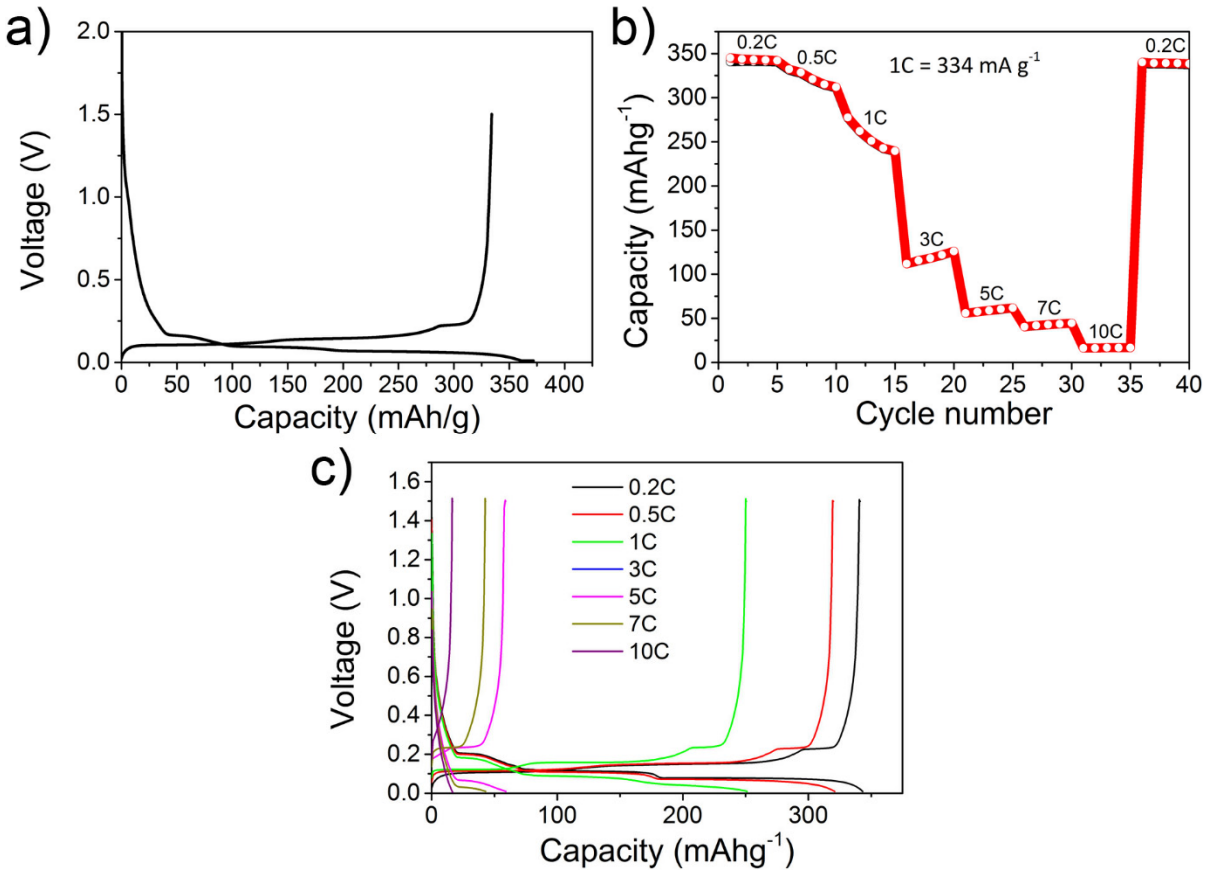

Figure S4. Electrochemical properties of natural graphite. a) Galvanostatic charge/discharge profile obtained under constant current at 0.05C, and constant voltage applied with 0.02 C at the end of process in the potential range of 1.5–0.01 V. b) Charge capacities at various charge rates from 0.2C to 10C. The discharge rates were fixed at 0.2C, but a constant voltage was applied with 0.05 C at 1.5 V. For various charge rates stepwise increased from 0.2 to 10C, the charge capacities of the natural graphite electrode dropped from 343 to 16 mAh g^{-1}. c) Voltage profiles of natural graphite at various charge rates from 0.2C to 10C. A rate of 1C corresponds to the current density of 334 mA g^{-1}.

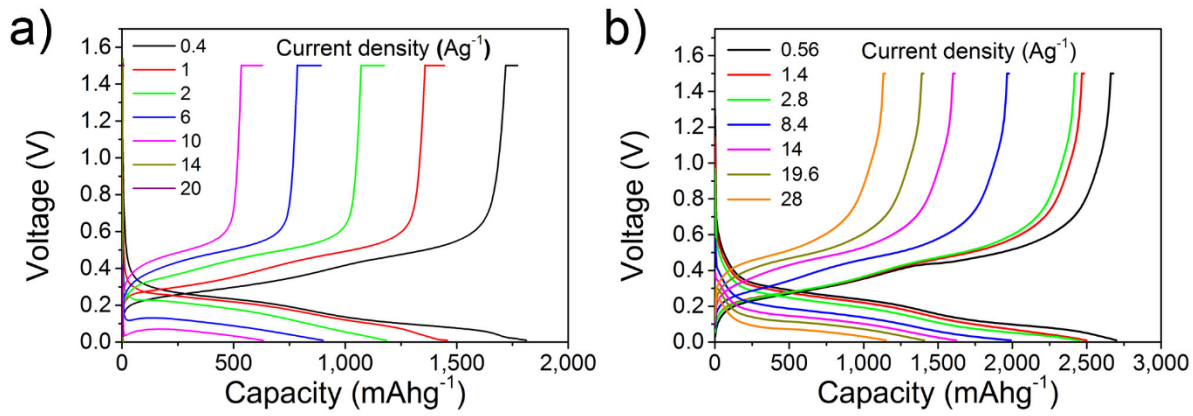

Figure S5. Voltage profiles for a) *a*-SBG and b) c-SiNP plotted for different charge current densities from 0.56 to 28 A g^{-1} and from 0.4 to 20 A g^{-1}, respectively.

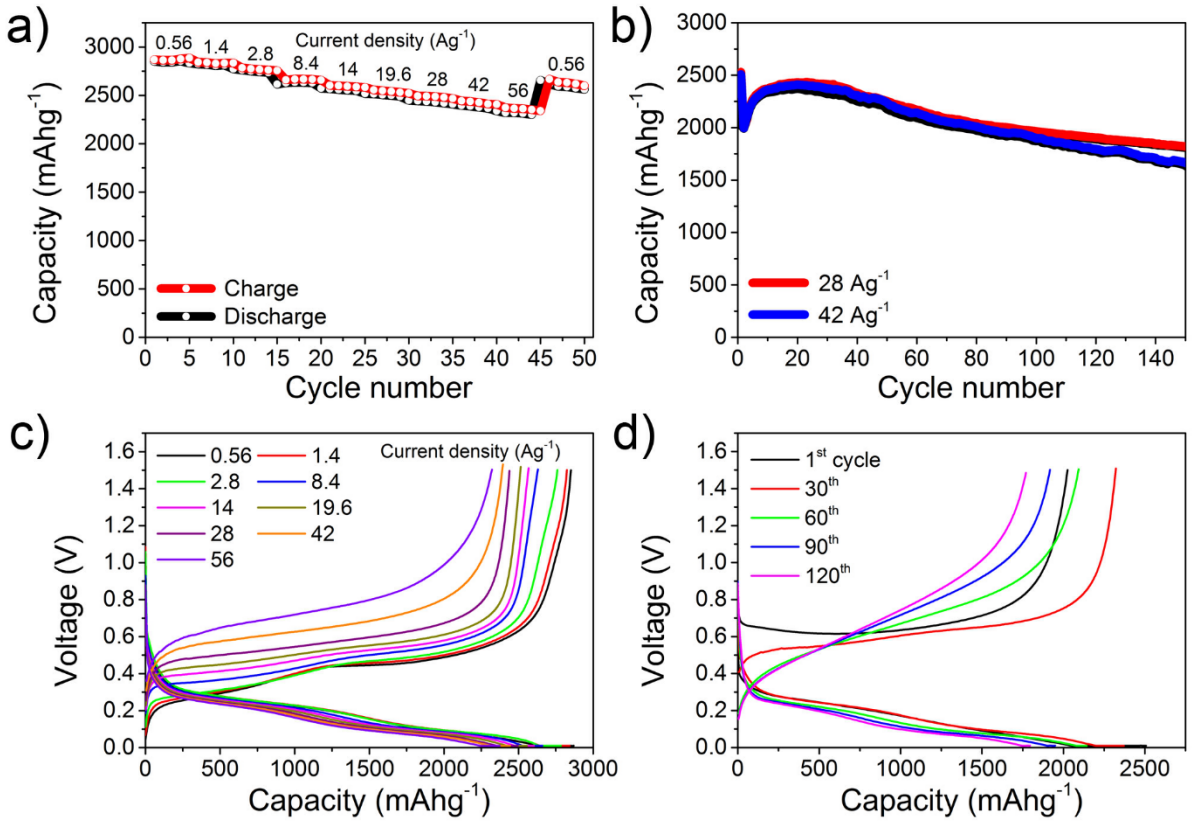

Figure S6. (a-d) Discharge performance of *a*-SBG nanocomposites in 2032R lithium half-cells at 24 °C. a) Capacity of *a*-SBG at various discharge current densities from 0.56 to 56 A g^{-1}. b) Cycling performance of *a*-SBG at discharge current density of 28 A g^{-1} and 42 A g^{-1} for 150 cycles. c) Voltage profiles of *a*-SBG as a function of discharge current density from 0.56 to 56 A g^{-1}. d) Voltage profiles of fast discharge cycling at 42 A g^{-1} plotted for 1st, 30th, 60th, 90th and 120th cycles. All electrochemical test were performed using a fixed charge current density of 1.4 A g^{-1}, but a constant voltage of 0.01 V was applied with 140 mA g^{-1} at the end of process.

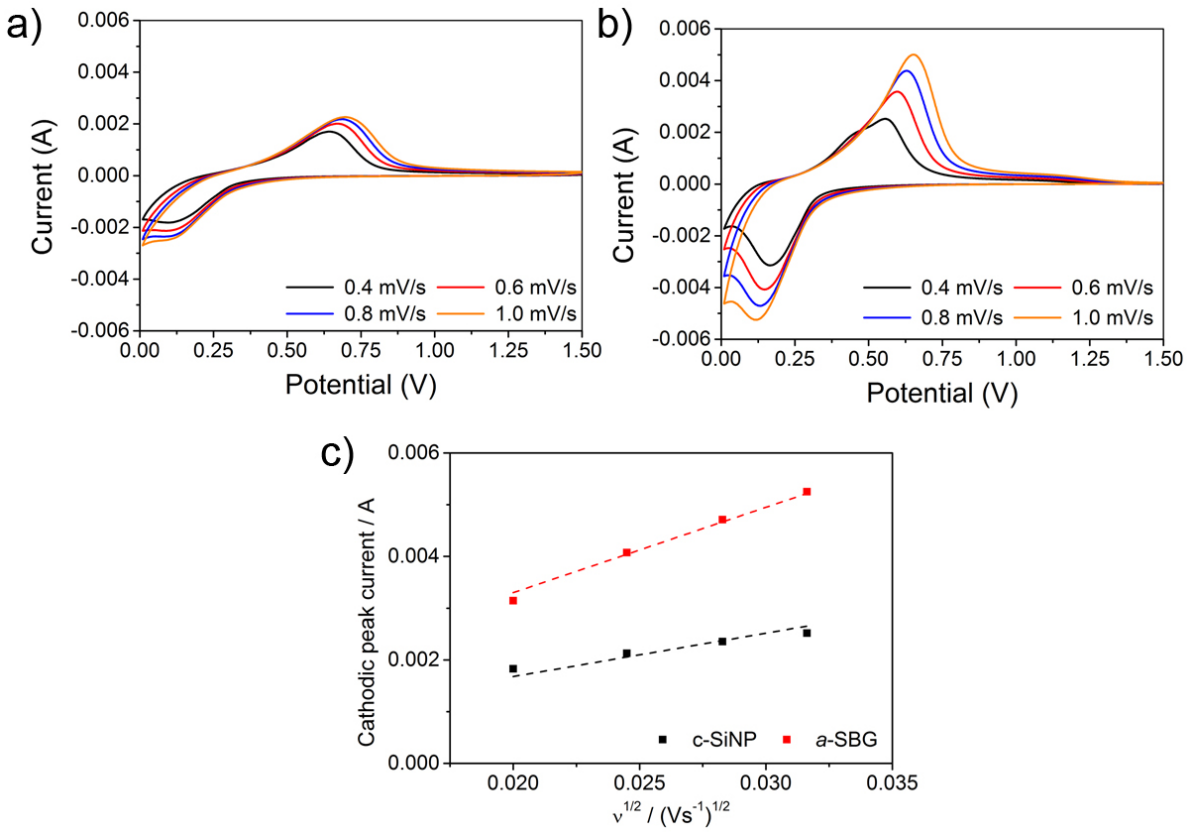

Figure S7. Cyclic Voltammetry for a) c-SiNP, and b) *a*-SBG electrode at various scan rates from 0.4 to 1.0 mV s^{-1} after initial cycle. c) The relationship between the cathodic peak current vs. the square root of the scan rate. The determination of apparent Li-ion diffusion coefficient by cyclic voltammetry: The coefficient was characterized by cyclic voltammetry (CV) with various scan rates from 0.4 to 1.0 mV s^{-1}. (a, b) the electrochemical results are well matched to silicon's behavior during cycling.[4, 5] Based on the results, (c) describes that the peak current is proportional to the square root of the scan rate, showing a linear plot. This analysis indicates that the rate-determining step, which is determined by variation from surface reaction to solid state diffusion of Li-ion, is controlled by semi-infinite diffusion of Li ion. The coefficient can be estimated by the following peak current equation:

$$I_p = (2.69 \times 10^5) n^{3/2} A D^{1/2} C_0 v^{1/2}$$

where n is the number of transferred electron (1 for Li^+), I_p is the peak current (ampere, A), A is the cross-section area of electrode (cm^2), D is the diffusion coefficient of Li ion ($cm^2\ s^{-1}$), C_0 is bulk concentration of Li ions, and v is the scan rate ($V\ s^{-1}$). In this work, the area of electrode reaction (A) was calculated to be 1.154 cm^2. The slope of *a*-SBG sample exhibited 2 times higher than that of silicon nanparticles (c-SiNP) resulting in the improvement of diffusion coefficient with ~4 times higher (*a*-SBG = 9.40×10^{-8} $cm^2\ s^{-1}$ / c-SiNP = 2.43×10^{-8} $cm^2\ s^{-1}$).

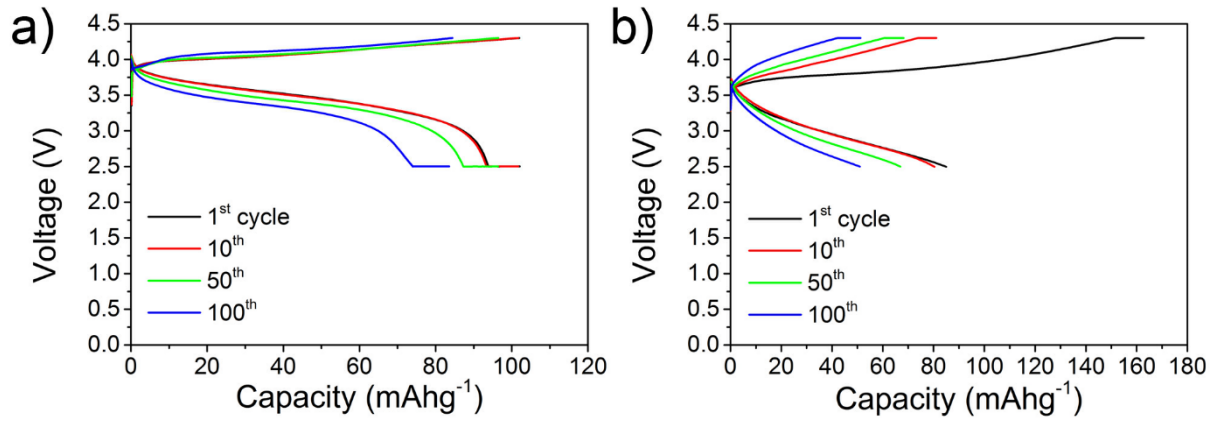

Figure S8. Voltage profiles for (**a**) 7C rate charge and (**b**) 20C rate discharge cycling for the 1st, 10th, 50th, and 100th cycles in full cell test.

■ REFERENCES

1. Ming, R.; Zhang, P.; He, X.; Feng, J.; Ding, Y.; Chang, F.; Wang, C. Humidity-Dependant Compression Properties of Graphene Oxide Foams Prepared by Freeze-Drying Technique. *Micro Nano Lett.* **2013**, 8, 66-67.
2. Fu, C. J.; Zhao, G. G.; Zhang, H. J.; Li, S. Evaluation and Characterization of Reduced Graphene Oxide Nanosheets as Anode Materials for Lithium-Ion Batteries. *Int. J. Electrochem. Sci.* **2013**, 8, 6269-6280.
3. Ganguly, A.; Sharma, S.; Papakonstantinou, P.; Hamilton, J. Probing the Thermal Deoxygenation of Graphene Oxide Using High-Resolution *in Situ* X-Ray-Based Spectroscopies. *J. Phys. Chem. C* **2011**, 115, 17009-17019.
4. Kulova, T. L.; Skundin, A. M.; Pleskov, Y. V.; Terukov, E. I.; Kon'kov, O. I. Lithium Insertion into Amorphous Silicon Thin-Film Electrodes. *J. Electroanal. Chem.* **2007**, 600, 217-225.
5. Pollak, E.; Salitra, G.; Baranchugov, V.; Aurbach, D. In Situ Conductivity, Impedance Spectroscopy, and Ex Situ Raman Spectra of Amorphous Silicon During the Insertion/Extraction of Lithium. *J. Phys. Chem. C* **2007**, 111, 11437-11444.